ANTIOXIDANTS & REDOX SIGNALING
Volume 9, Number 12, 2007

DOI: 10.1089/ars.2007.1791

Forum Original Research Communication

Cell Stress Induced by the Parkinsonian Mimetic, 6-Hydroxydopamine, is Concurrent with Oxidation of the Chaperone, ERp57, and Aggresome Formation

JEONG SOOK KIM-HAN and KAREN L. O'MALLEY

ABSTRACT

Parkinson's disease (PD) involves an irreversible degeneration of the nigrostriatal pathway. As most cases of PD are sporadic, environmental risk factors may underlie neurodegeneration in dopaminergic neurons. One such factor is 6-hydroxydopamine (6-OHDA), which is widely used as a parkinsonian mimetic. Studies have shown that 6-OHDA generates reactive oxygen species and induces cell stress, the unfolded protein response, and apoptosis. Present findings show that 6-OHDA, but not hydrogen peroxide, MPP^+, or rotenone, leads to the rapid formation of high-molecular-weight species of protein disulfide isomerase–associated protein 3 (ERp57) in a dose- and time-dependent fashion. Moreover, ERp57 conjugates are blocked by *N*-acetylcysteine and glutathione, suggesting that they represent oxidized forms of protein. Surprisingly, conjugates are complexed with DNA, because treatment with DNase reduces their appearance. Subcellular fractionation indicates that both nuclear and mitochondrial DNA are associated with the protein. Finally, toxin-treated ERp57 rapidly forms juxtanuclear aggresome-like structures in dopaminergic cells, suggesting that ERp57 plays an early adaptive response in toxin-mediated stress. Understanding the signaling mechanisms associated with parkinsonian mimetics, as well as their temporal induction, may aid in designing better interventions in models of PD. *Antioxid. Redox Signal.* 9, 2255–2264.

INTRODUCTION

Numerous studies suggest that cellular stress systems are involved in a variety of neurodegenerative disorders such as Alzheimer's disease, Parkinson's disease (PD), and prion-related disorders. In particular, genetic mutations linked to PD, such as α-synuclein, parkin, UCH-L1, and LRRK2, have highlighted the role of aberrant protein degradation in this disorder (11). Accumulation of protein aggregates within the cell can trigger stress-activated signaling pathways, particularly in the endoplasmic reticulum (ER), which in turn activate adaptive responses such as the unfolded protein response (UPR). The UPR-mediated recovery from ER stress uses both protein translation and gene transcription to overcome abnormal protein alterations. Prolonged cell stress, however, overwhelms these processes, and apoptosis is initiated (43). Previous results from this laboratory (13–15), as well as others (*e.g.*, 36), demonstrated a link between PD-associated genetic and environmental factors with the discovery that the widely used parkinsonian mimetic, 6-hydroxydopamine (6-OHDA) induces the upregulation of genes involved in the ER stress response. Mechanistically, 6-OHDA–induced reactive oxygen species (ROS) lead to the rapid formation of oxidized, carbonylated proteins that precede UPR upregulation (14).

Evidence suggests that carbonylation is a common indicator of oxidative damage in aging and in neurodegenerative disorders, such as PD (32). In general, however, only subsets of proteins have been shown to be carbonylated, such as chaperones,

Department of Anatomy and Neurobiology, Washington University School of Medicine, St. Louis, Missouri.

cytoskeletal proteins, protein disulfide isomerases (PDIs), and various metabolic enzymes (1, 5, 7, 34). Oxidation of these proteins, many of which are cell protective, may trigger downstream events such as UPR and apoptosis. Previously, we reported that one such carbonylation-prone protein, PDI-associated protein 3 (ERp57; Genebank MGI:95834), was upregulated by 6-OHDA (13).

ERp57 (or GRP58) was first reported as a glucose-regulated protein/chaperone along with other cell-stress proteins like GRP78(BIP) and GRP94 (23, 26). Largely localized in the ER lumen, ERp57 not only plays a role as a chaperone but it also functions as a disulfide reductase, a disulfide isomerase, and a dithiol oxidase (10). Recently, ERp57 was shown to be upregulated after prion replication in a murine scrapie model, in which it appeared to serve a neuroprotectant role (12). As scrapie and other transmissible spongiform encephalopathies are characterized by the accumulation of abnormally folded prion protein, these data suggest that ERp57 somehow plays a role in abrogating these processes. Whether ERp57 blocks some step in this process or helps to prevent prion aggregation in the first place (or both) is unclear.

One early step in protein aggregation is the formation of so-called aggresomes. These clusters of aggregated proteins are retrogradely transported on microtubules to juxtanuclear regions where they can be degraded by autophagy (21). Typically, aggresomes are enriched in chaperones, 19S and 26S proteasome subunits, intermediate filament proteins, and ubiquitin (21). Although autophagic vesicles are considered a cellular defense mechanism, they can lead to cell death by interfering with normal cellular trafficking or by incomplete degradation of aggregated material. The latter may overwhelm the ubiquitin–proteosome system, triggering ER stress, UPR, and apoptosis. (31). Thus, emerging studies suggest links between ER stress, protein aggregation, and autophagy (16, 29, 35). These findings, together with the upregulation of ERp57 in dopaminergic cells after toxin treatment, prompted us to test the hypothesis that ERp57 plays a role in 6-OHDA–mediated UPR induction. Here we show that toxin-treated dopaminergic cells lead to the rapid appearance of DNA-containing high-molecular-weight conjugates of ERp57 as well as aggresome formation. These data suggest that ERp57 plays an early adaptive response in 6-OHDA–mediated toxicity.

MATERIALS AND METHODS

Materials and reagents

Rabbit anti-ERp57 antibody was kindly provided by Dr. Thomas Wileman (Institute for Animal Health, Surrey, U.K.). RNase A and Complete protease inhibitor mixture were purchased from Roche (Mannheim, Germany). Unless otherwise indicated, all other chemicals were from Sigma (St. Louis, MO).

Cell cultures

Murine primary mesencephalic neuronal cultures were prepared as described previously (25). In brief, the ventral mesencephalon was dissected from embryonic day 14 CF1 murine embryos (Charles River Laboratories, Wilmington, MA). Tissues were trypsinized in the presence of 0.05% DNase and triturated by using a Pasteur pipette. Dissociated cells (1.5×10^6 cells/cm^2) were plated on the 0.5-mg/ml poly-D-lysine and 2.5 μg/ml laminin (BD Bioscience, San Jose, CA) precoated culture dishes. Cultures were used 7–9 days after plating.

MN9D cells, an immortalized murine mesencephalic dopaminergic cell line (4), were plated on 0.1 mg/ml poly-D-lysine precoated plates and maintained in Iscove's Dulbecco's modified Eagle's medium with 10% fetal bovine serum in the presence of 10% CO_2 at 37°C. Medium was replaced with serum-free Iscove's Dulbecco's modified Eagle's medium/F12/B27 supplement 30 min before the addition of experimental agents.

Western blot analysis

After treatment, samples were washed twice with phosphate-buffered saline (PBS), lysed in RIPA buffer (50 m*M* Tris-HCl, pH 7.5; 1% NP-40; 1% deoxycholate; 0.1% SDS; 150 m*M* NaCl) and Complete protease inhibitor mixture and pelleted by centrifugation. The supernatant was collected. Protein concentrations were measured by the BioRad Protein Assay Kit (Hercules, CA) by using bovine serum albumin as a control. Equal amounts of protein were then run on 12% polyacrylamide gels and transferred onto PVDF membranes (BioRad). After incubation in blocking buffer (20 m*M* Tris base, 150 m*M* NaCl, 5% nonfat milk, and 0.1% Tween 20), membranes were incubated with primary antibodies overnight at 4°C. ERp57 protein was detected with a polyclonal rabbit anti-human ERp57 antibody at a dilution of 1:2,000. Mouse monoclonal antibodies against β-actin (Sigma; 1:5,000), calnexin (BD Bioscience, San Jose, CA; 1:250), cytochrome *c* (BD Pharmingen, San Diego, CA; 1:500), lamin B (Zymed, South San Francisco; 1:1,000), and STAT3 (Cell Signaling, Danvers, MA; 1:1,000) were used.

After washes in the blocking buffer, membranes were incubated for 1 h with the appropriate anti-IgG secondary antibody conjugated to horseradish peroxidase (Cell Signaling) diluted 1:3,000. After a second series of washes, bound antibody complexes were visualized by using the ECL plus Western Blotting Detection System ECL (GE Healthcare, Buckinghamshire, U.K.) and quantitative fluoroimaging (Storm 860; Global Medical Instrumentation, Inc., Ramsey, MN).

Immunocytochemistry

After treatment, cells were rinsed twice with PBS, fixed with 4% paraformaldehyde in PBS for 30 min. Cells were double-stained with anti-ERp57 antibody (1:2,000) and cytochrome *c* (Promega, Madison, WI; 1:4,000) or LAMP1 (Hybridoma 1D4B, Developmental Studies Hybridoma Bank, The University of Iowa, Iowa City, IA; 1:100) antibody, together with a sheep polyclonal antibody against the dopaminergic neuronal marker, tyrosine hydroxylase (Novus Biologicals, Littleton, CO; 1:600). Mouse monoclonal antibodies against γ-tubulin (Sigma; 1:10,000), and 8-hydroxyguanosine (QED Bioscience, San Diego, CA; 1:100) were used. Secondary antibodies conjugated with Cy3 (anti-mouse and anti-rabbit, 1:300; Jackson ImmunoResearch Laboratories, West Grove, PA) and Alexa 488 (anti-mouse, 1:500; anti-rabbit, 1:2,000; Molecular Probes, Eugene, OR) were used. Cells were imaged by using an Olympus Fluoview confocal microscope.

Treatment of lysates with DNase or RNase

Cell lysates were treated with 10 mg/ml DNaseI or 10 mg/ml RNase or both in 10 m*M* Tris-HCl, pH 7.0, 2.5 m*M* $MgCl_2$, and 0.5 m*M* $CaCl_2$ at 25°C for 1 h. Samples were subjected to SDS-PAGE, followed by Western blot analysis.

Subcellular fractionation

Cells were rinsed and harvested in PBS and homogenized in a sucrose buffer (0.32 *M* sucrose, 10 m*M* Tris-HCl, pH 7.2; 1 m*M* EDTA, pH 8.0) containing Complete protease inhibitors by using an all-glass Dounce homogenizer. After centrifugation at 800 *g* for 5 min, the supernatant was centrifuged at 10,000 *g* for 10 min. Pellets were collected for the mitochondrial fraction (M), and the supernatant was further centrifuged at 100,000 *g* for 1 h to obtain microsomal membranes (ER) and cytosol (C). All fractions were resuspended in RIPA buffer and subjected to Western blot analysis.

Determination of redox state of ERp57 in vivo

The redox state of ERp57 *in vivo* was determined by sequential alkylation of free thiols with *N*-ethylmaleimide (NEM) and 4-acetamido-4′-maleimidylstilbene-2,2′-disulfonic acid (AMS), essentially as described by Jessop and Bulleid (19), but with some minor modifications. In brief, cells were treated with 25 m*M* NEM for 20 min at 37°C, washed with ice-cold PBS, and lysed in 50 m*M* Tris-HCl, pH 7.5, 150 m*M* NaCl, 2 m*M* EDTA, 1× Complete protease inhibitor mixture, and 1% Triton X-100. Cell lysates were treated with 2% SDS and 50 m*M* DTT, precipitated with 10% trichloroacetic acid, washed with ice-cold 70% acetone, and resuspended in 80 m*M* Tris, pH 6.8, 2% SDS, and 1× Complete protease inhibitor mixture. Samples were incubated with 30 m*M* AMS overnight at 25°C followed by 20 min at 37°C. Samples were separated by 7.5–12.5% gradient SDS-PAGE and Western blotted to detect ERp57. To determine the "all-oxidized" or "all-reduced" form of ERp57, cells were treated with 5 m*M* dipyridyl sulfide (DPS) or 10 m*M* dithiothreitol (DTT), respectively, for 5 min before the addition of alkylating thiols.

RESULTS

ERp57 is partially oxidized in MN9D cells

Previously we showed that 6-OHDA rapidly induces ER stress and UPR in MN9D and primary dopaminergic neurons in a ROS-dependent fashion (13). As ERp57 was one of 21 proteins specifically upregulated by 6-OHDA (13) and because it is readily oxidized (22), we tested the hypothesis that ERp57 is specifically oxidized by toxin treatment in MN9D cells. Cells were treated with and without 6-OHDA for 3 h, after which cell lysates were alkylated to determine the oxidation state of ERp57. Although most reports describe ERp57 as primarily being reduced (20), equal amounts of oxidized and reduced forms of ERp57 were observed in MN9D cells, even in nontreated cells (Fig. 1A and B). Surprisingly, toxin treatment did not alter these ratios (Fig. 1A and B). Co-treatment with the thiol antioxidant, *N*-acetyl-L-cysteine (NAC) significantly increased the reduced form of ERp57, irrespective of the presence of 6-OHDA. Therefore, ERp57 is already partially oxidized in nontreated, control MN9D cells.

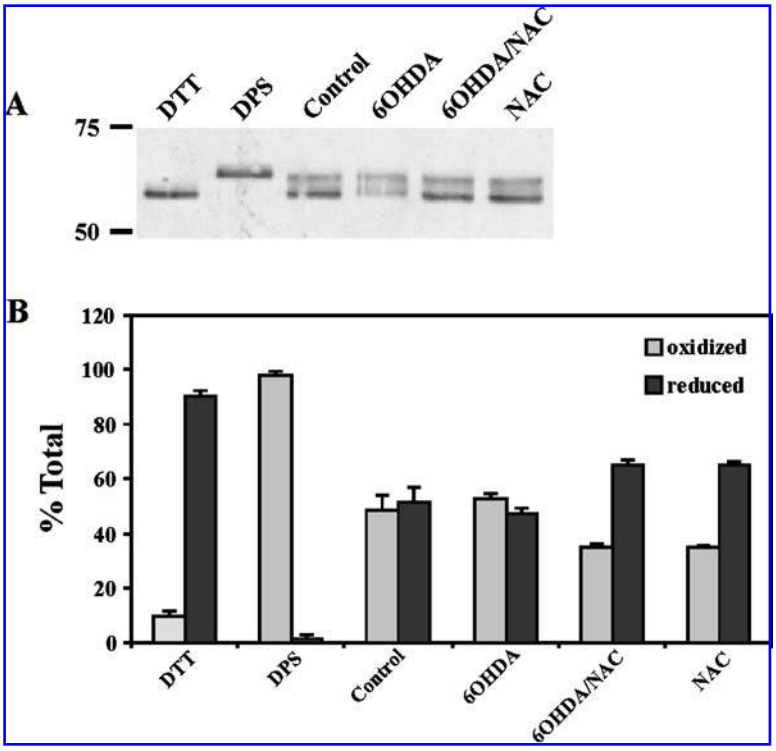

FIG. 1. 6-OHDA does not alter the ratio of oxidized to reduced ERp57 in MN9D cells. (**A**) Cells were treated as indicated before NEM alkylation and lysis. After an overnight incubation with AMS, cell lysates were subjected to gradient SDS-PAGE and Western blotting with antibodies against ERp57. Samples treated with DTT or DPS for 5 min before fixation were used to determine the reduced and oxidized states of ERp57. (**B**) Quantitation of results shown in (**A**). Values represent mean ± SEM, $n = 3$.

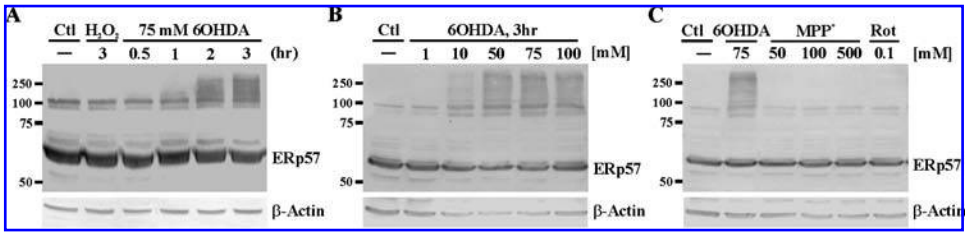

FIG. 2. 6-OHDA induces the formation of HMW conjugates of ERp57. MN9D cells were treated as indicated, and cell lysates were prepared for Western blotting with anti-ERp57 antibodies. Time- (**A**) and dose (**B**)-dependent appearance of ERp57 HMW conjugates induced by 6-OHDA but not 1 m*M* H_2O_2. (**C**) Neither MPP^+ nor rotenone (Rot) formed HMW conjugates 3 h after treatment, as indicated. Ctl, control.

6-OHDA treatment results in the rapid formation of high-molecular-weight conjugates of ERp57

Although 6-OHDA did not alter the oxidation state of ERp57 in MN9D cells, Western blot analysis revealed the unexpected formation of high-molecular-weight (HMW) conjugates shortly after toxin treatment in MN9D cells (Fig. 2A). Specifically, HMW conjugates were first visible at 1 h after 6-OHDA treatment, reaching a maximum at 3 h, and persisting for at least 12 h, the longest time point tested (Figs. 2A and 3A). The formation of HMW conjugates was dose dependent (Fig. 2B) and specific for 6-OHDA, because other compounds known to generate ROS, such as H_2O_2, MPP^+, or rotenone never formed HMW species at any concentration tested (Fig. 2A and C). To identify the location of HMW conjugation, subcellular fractionation was performed after treatment with 6-OHDA. Contrary to most reports, in MN9D cells, ERp57 was highly expressed in the mitochondrial fraction (Cox I positive fraction) *versus* ER membranes (P100; Fig. 3A) or the cytosol (S100; Fig. 3A). HMW conjugates were enriched in the mitochondrial fractions at all times (Fig. 3A). To determine whether the HMW conjugates represented ERp57 covalent interactions stabilized by disulfide bridges, lysates were treated with a reducing agent before size fractionation and Western blotting. Because no change in band intensity was observed in the presence of the reducing agent (Fig. 3B), it seems unlikely that the HMW species represent ERp57 oligomers linked by disulfide bonds. Taken together, these data indicate that the dopaminergic toxin, 6-OHDA, induces a specific change in ERp57 that leads to the rapid induction of HMW conjugates of unknown function.

Toxin-induced ERp57 HMW conjugates contain DNA

To test whether the formation of HMW ERp57 conjugates by 6-OHDA could be blocked by antioxidants, MN9D cells were co-treated with NAC or glutathione in the presence of toxin. NAC completely abolished the HMW ERp57 conjugates, whereas glutathione only partially blocked their appearance (Fig. 4A). To test whether the HMW ERp57 species were complexes of known ERp57-interacting proteins, Western blots were probed with antibodies directed against the transcription factor, STAT3, or calnexin. No specific bands were revealed, however, in the size range of the ERp57 HMW conjugates after 6-OHDA treatment (data not shown). Similarly, treatment with deglycosylation agents such as PNGF did not shift the size range of the HMW conjugates (Fig. 4B). Surprisingly, treatment of protein lysates with DNaseI significantly decreased the levels of 6-OHDA–generated HMW conjugates, whereas inclusion of RNase did not induce any

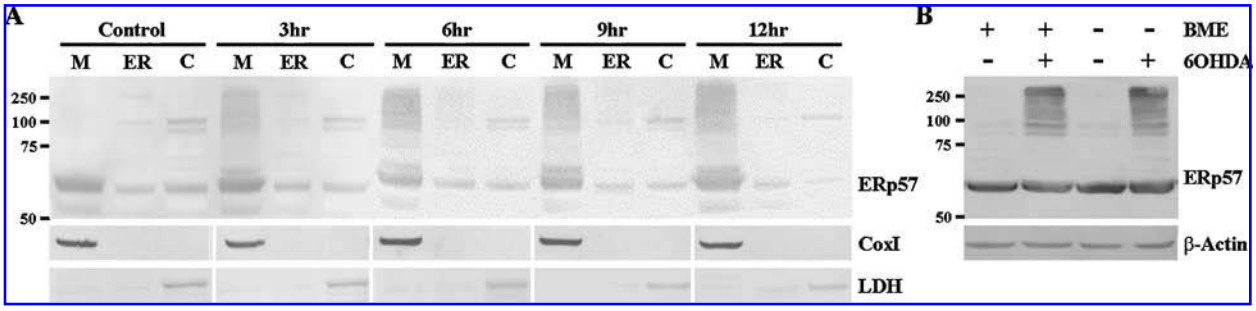

FIG. 3. Characterization of HMW conjugates of ERp57 induced by 6-OHDA. MN9D cell lysates after treatment, as indicated, were prepared for Western blotting with anti-ERp57 antibodies. (**A**) Subcellular fractionation of MN9D cells was performed to obtain mitochondrial (M), ER, and cytoplasmic (C) fractions from untreated cells or cells treated for 3, 6, 9, or 12 h with 75 μM 6-OHDA. Fractions were Western blotted with anti-CoxI and anti-LDH confirming compartmental designations as well as anti-ERp57 to detect changes in localization. Results shown are representative of at least three independent experiments. (**B**) HMW conjugates were not affected by the reducing agent, β-mercaptoethanol (BME). Protein samples were treated with or without BME before SDS-PAGE. Where indicated, β-actin served as a loading control.

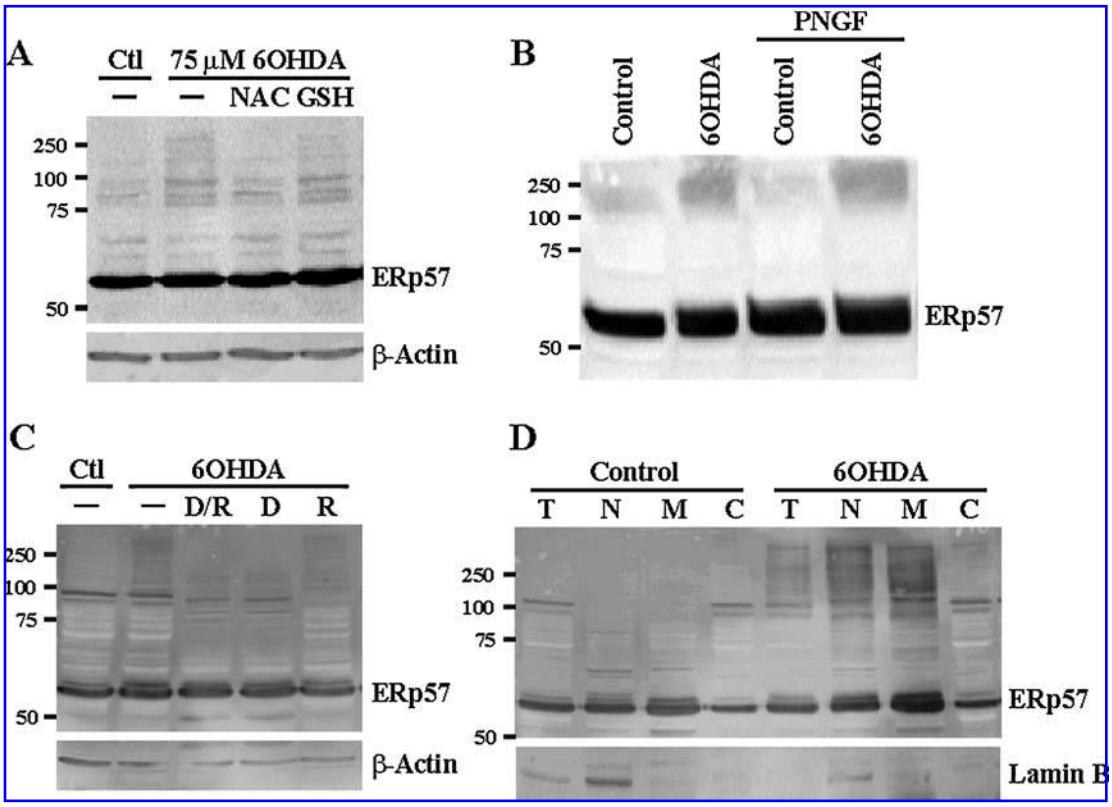

FIG. 4. ERp57 HMW conjugates are complexed with DNA. (**A**) HMW conjugates can be blocked by cotreatment of antioxidants NAC (5 m*M*) and glutathione (1 m*M*). (**B**) HMW conjugates are not glycosylated because inclusion of peptide *N*-glycosidase F (PNGF) did not change their mobility. (**C**) Treatment of protein lysates with DNase (D) but not RNase (R) before loading the gel significantly reduces the intensity of HMW conjugates. (**D**) Subcellular fractionation shows that the HMW conjugates are present in both nuclear (N) and crude mitochondrial (M) fractions. (T, total cell lysates; C, cytosol). LaminB was used as a marker for the nuclear fraction. Results shown are representative of at least three independent experiments.

changes (Fig. 4C). To identify the possible source of DNA, subcellular fractionation was performed after treatment with 6-OHDA. ERp57 HMW conjugates were enriched in both nuclear and mitochondrial fractions and essentially absent from cytosolic fractions (Fig. 4D). These data suggest that ERp57 can form HMW complexes with either nuclear or mitochondrial DNA.

ERp57 forms juxtanuclear clusters after 6-OHDA treatment in MN9D cells

To identify the location of ERp57 *in situ* before and after toxin treatment, cells were fixed and immunostained with anti-ERp57 antibody. The overall level of ERp57 expression did not appear to change at 5 h, although its distribution coalesced over time into a doughnut-shaped structure in the cytosol near the nucleus (Fig. 5A). Toxin-induced ERp57 clusters co-localized with cytochrome *c* (Fig. 5A). Because this timepoint precedes cytochrome *c* release from mitochondria (14), these data suggest that mitochondria were also clustering in the juxtanuclear region. Quantification of cells with ERp57 clusters revealed significantly higher numbers in treated *versus* nontreated cells 3 and 5 h after 6-OHDA treatment (Fig. 5B). With the same experimental paradigm, toxin-treated ERp57 clusters encircled the lysosomal marker, LAMP1 [Fig. 6A (8)] but not G58 (a golgi marker), β-actin (a cytoskeletal marker), γ-tubulin (microtubule-organizing center), or 8-hydroxyguanosine (DNA/RNA oxidative damage marker; not shown). When the percentage of the cytosolic area stained with LAMP1 is quantified, a significant drug effect is observed (Fig. 6B). These distinctive structural changes are reminiscent of aggresomes (21).

ERp57 is primarily reduced in dopaminergic neurons

To confirm and extend these results in primary dopaminergic neurons, the redox state of ERp57 in dissociated cultures was examined. Unlike MN9D cells, primary dopaminergic neurons exhibited a significantly higher level of reduced *versus* oxidized ERp57 before toxin treatment (Fig. 7A and B). Incubation with 6-OHDA increased oxidized ERp57 monomers, significantly altering the ratio between reduced and oxidized ERp57 (Fig. 7B). Co-treatment with NAC prevented these changes (Fig. 7A and B). Toxin treatment also induced the formation of HMW ERp57 conjugates, albeit to a lesser extent than those seen in MN9D cells (Fig. 8A). Neither MPP^+ nor rotenone induced the formation of conjugates (Fig. 8A). Therefore, like MN9D cells, ERp57 specifically responds to 6-OHDA

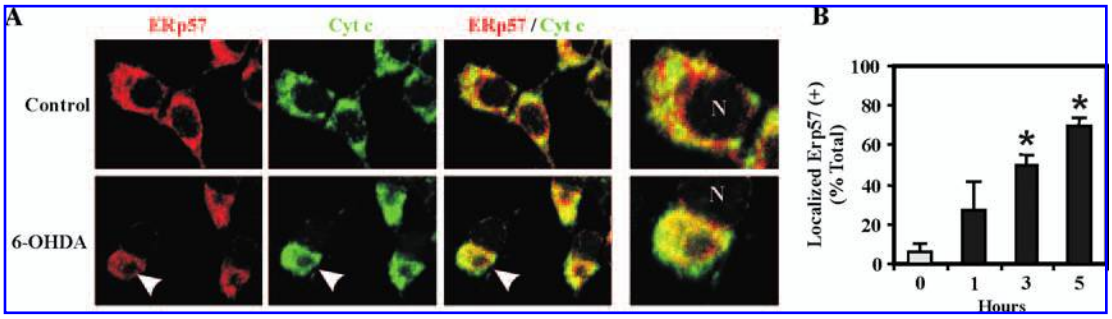

FIG. 5. ERp57 forms juxtanuclear clusters after toxin treatment of MN9D cells. (**A**) ERp57 immunostaining of control cells reveals a punctuated intracellular distribution that, in most cases, does not overlap with cytochrome *c* (Cyt c; mitochondria). After 6-OHDA (75 μM) treatment, ERp57 coalesces into doughnut-shaped structures (*arrowheads*) near the nucleus (N), which overlap with cytochrome *c*. (**B**) Changes in ERp57 distribution were quantified as described in Methods. *$p < 0.05$ by one-way ANOVA with *post hoc* Tukey's test.

although the cellular environment of mesencephalic neurons appears to be less oxidizing.

6-OHDA also leads to ERp57 juxtanuclear clustering in primary mesencephalic neurons

To determine whether ERp57 formed toxin-induced aggregates, cultures were treated with and without 6-OHDA and examined for the appearance of clusters. Confocal microscopy revealed toxin-induced ERp57 juxtanuclear clustering in dopaminergic neurons 6 h after treatment (Fig. 8B). At this time, many UPR markers have been upregulated as well as showing early signs of apoptosis (13–15, 25). Thus, the apparent shrinkage of neurons and nuclei (Neu N staining) after toxin treatment was consistent with our previous findings that 6-OHDA–mediated cell death proceeds *via* UPR upregulation and downstream apoptosis.

DISCUSSION

A growing body of evidence suggests that ER stress-triggered UPR is an important component of many neurodegenerative disorders. Previous results from this laboratory and others have shown that the parkinsonian mimetic, 6-OHDA, induces UPR and subsequently apoptosis in the dopaminergic cell line, MN9D, as well as in primary dopaminergic neurons. Here we show that one such induced UPR marker, ERp57, rapidly forms toxin-specific HMW conjugates with DNA as well as juxtanuclear clusters of protein. As both structures form before the induction of apoptosis in these cells (14), these data suggest that they represent adaptive responses to toxin-mediated UPR.

Although 6-OHDA has been used as a model of PD for over 30 years, its mechanisms of action are still unclear. Readily autooxidized, 6-OHDA produces many types of ROS, including hydrogen peroxide, superoxide, and quinone derivatives, which are responsible for its toxicity. Previously we showed that, before the appearance of UPR markers, 6-OHDA–generated ROS can be rapidly detected in MN9D cells (14) as well as primary dopaminergic neurons (25). Because ROS formation was quickly followed by the appearance of oxidized proteins and UPR but not release of cytochrome *c*, these data suggested that death induced by parkinsonian toxins first initiated ER stress mechanisms and then the mitochondrial apoptotic machinery (14). Surprisingly, obvious oxidation sensors, such as the ASK1/MAP kinase signaling pathway associated with the UPR gatekeeper, IRE1 (39), or the mitochondrial permeability

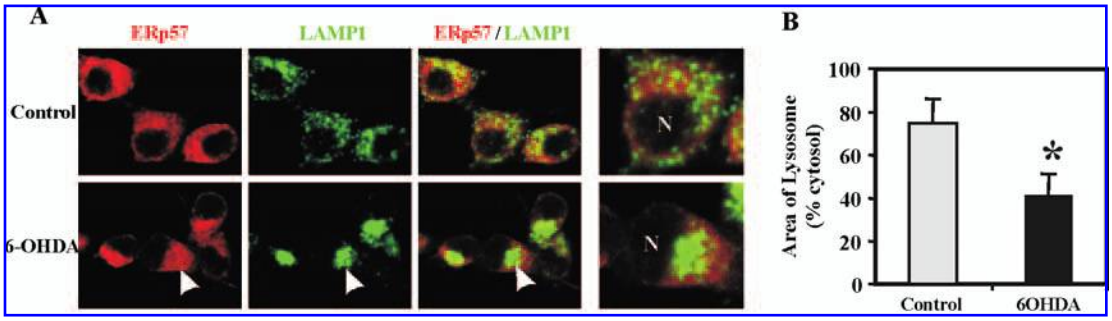

FIG. 6. ERp57 coalesces around LAMP1 after toxin treatment of MN9D cells. (**A**) ERp57 immunostaining of control cells is largely independent of LAMP1 (lysosomes). LAMP1 redistributes to the center of the doughnut-shaped structure (*arrows*). N, nucleus. (**B**) When the percentage of the cytosolic area is quantified for LAMP1, a significant drug effect is observed (*$p < 0.001$ by Student's *t* test).

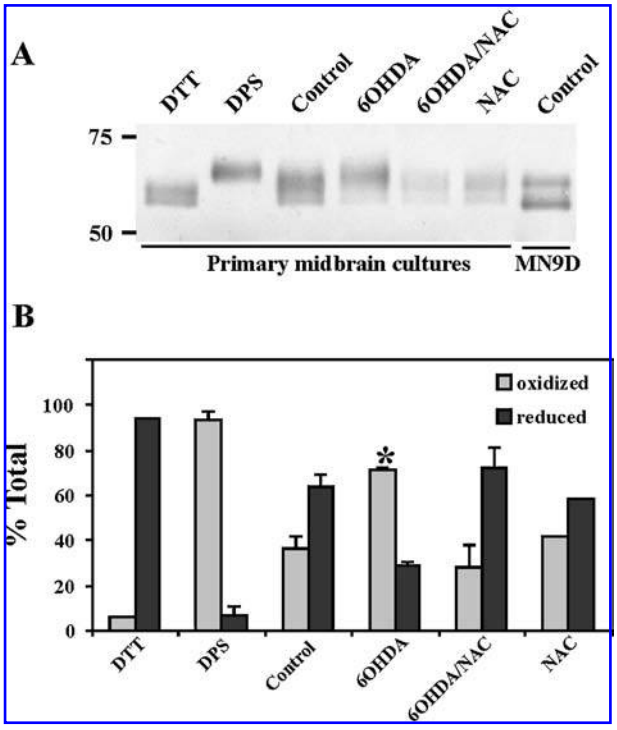

FIG. 7. 6-OHDA induces ERp57 oxidation in mesencephalic neurons. (**A**) Cells were treated with or without indicated dose of 6-OHDA for 3 h before NEM alkylation and lysis. Some samples were pretreated with 5 m*M* NAC. After AMS treatment, cell lysates were subjected to gradient SDS-PAGE and Western blotting with antibodies against ERp57. Samples treated with DTT or DPS for 5 min before fixation were used to determine the reduced and oxidized states of ERp57 in primary mesencephalic cultures. Nontreated MN9D cell lysates were included as a reference. (**B**) Quantitation of results shown in (**A**). Values represent mean ± SEM, $n = 3$. *$p < 0.05$ by one-way ANOVA with Tukey's test.

pore, or disruption of ER calcium homeostasis, were not associated with 6-OHDA–mediated cell death [(14), and JSKH, unpublished data). Instead, protein oxidation is one of the first events after 6-OHDA–generated ROS, in particular, changes in the protein disulfide isomerase, ERp57, appear early in this process (see Fig. 2). Because ERp57 has been shown to be neuroprotective in models of prion-related disorders (12), its oxidation may trigger downstream sequelae such as UPR and apoptosis. Whether knockdown or loss of ERp57 accelerates 6-OHDA–mediated cell death or its enforced expression blocks toxin effects remains to be tested in this system.

6-OHDA-induced high-molecular-weight conjugates of ERp57

What is the nature of the HMW conjugates involving ERp57? As no differences were observed in band intensity when lysates were treated with a reducing agent before size fractionation and Western blotting (see Fig. 3B), it seems unlikely that the HMW species represent covalent interactions stabilized by disulfide bridges. Numerous studies, however, have shown that reactive quinone species, such as diethylstilbesterol quinone, 4-hydroxytamoxifen, and/or tocopherol quinine, form covalent quinone-linked bonds with either free sulfhydryl groups or DNA (40, 47). As described, oxidation of 6-OHDA leads to quinone formation (17, 38), as does dopamine itself (41). Inasmuch as H_2O_2 does not replicate the cell-death paradigms we have observed (14; this work), we would suggest that it is 6-OHDA–generated quinone species that are triggering ER stress, UPR, protein carbonylation, *etc*. (14). In support of this notion, recent data investigating tocopherol quinone toxicity demonstrated a direct link with ER stress and subsequent cell death (47). These authors suggested that quinone-mediated covalent bonding with ER PDIs triggered this response (47). Taken together, our data support a model in which 6-OHDA–generated quinone species form covalent ERp57/DNA adducts that precede the appearance of ER stress and apoptotic markers.

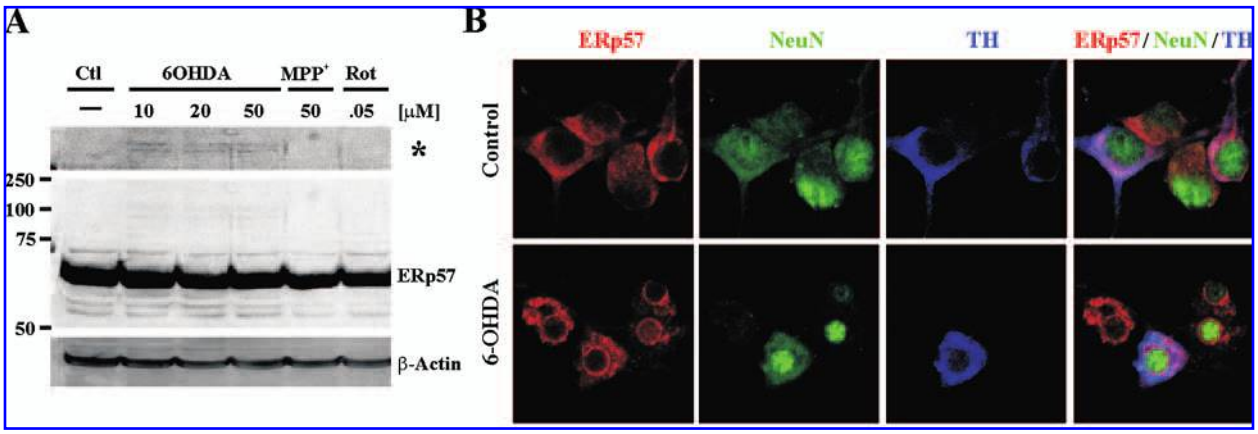

FIG. 8. 6-OHDA induces HMW conjugates and juxtanuclear clustering of ERp57 in mesencephalic neurons. (**A**) 6-OHDA but not MPP^+ or rotenone (Rot) induced HMW ERp57 conjugates in mesencephalic cultures. β-actin served as a loading control. *Longer exposure of middle panel. (**B**) DIV 7 mesencephalic cultures were treated with and without 20 μM 6-OHDA for 6 h before fixation. Neuronal and dopaminergic cells were identified with anti-NeuN and anti-TH antibodies, respectively. Toxin treatment induced the redistribution of ERp57 to a juxtanuclear position. Also at this time, NeuN appears condensed within the nucleus.

ERp57 in the nucleus and mitochondria

In general, ERp57 is largely confined to the lumen of the ER, although detectable levels of expression have been found in the cytosol and the nucleus (44). Within the ER, ERp57 is thought to form a non-covalent complex with the lectin-like chaperones, calreticulin and calnexin, to promote the correct folding of various glycoproteins (48). In the cytosol, ERp57 was identified as a cytokine-dependent STAT3-associated protein serving as a chaperone in the transit of STAT3 from the cell membrane to the nucleus (30). Interestingly, in dopaminergic cells, ERp57 is not abundantly expressed in either the ER or the cytosol. Rather, the present study demonstrates that ERp57 is highly associated with mitochondrial fractions (see Figs. 3 and 4). More ERp57 is associated with this fraction than with any other. Further characterization of mitochondrial fractions by using sucrose gradients suggests that ERp57 is most highly enriched in the mitochondria-associated membrane (MAM) fraction (data not shown), a region in which the ER membrane is juxtaposed to the mitochondria. The so-called MAM fraction is responsible for the transport of phospholipids from ER to mitochondria (42). It will be of interest to test whether ERp57 plays a role in phospholipid cycling.

In the nucleus, ERp57 catalyzes the attachment of DNA loops to matrix proteins (6), binds specific DNA sequences associated with, among other things, scaffold/matrix-associated regions (3), and is recruited when various antitumor agents such as mitomycin C crosslink DNA (2). Mitomycin-induced DNA damage is thought to be due to its propensity to form highly reactive quinone derivatives that can alkylate DNA and cross link individual strands (46). As H_2O_2 did not induce HMW conjugates of ERp57 (see Fig. 2A), conceivably these can be ascribed to 6-OHDA quinone formation, which has been associated with its cytotoxicity [*e.g.*, (17)]. Therefore, it seems likely that 6-OHDA not only oxidizes proteins (14) but also damages DNA, potentially triggering the ERp57 response. In support of this notion, studies have reported that 6-OHDA produces DNA adducts and base alterations in cell lines and *in vivo* (9, 24). It is unclear, however, what DNA sequences are involved in this response and how and why mitochondrial DNA is affected as well. Moreover, it is unclear whether ERp57 is recruited from the cytosol or from membranous structures. Finally, DNA damage will initiate other adaptive cellular responses, including activation of DNA-repair systems, blockade of cell-cycle progression, transcriptional activation, and when all else fails, apoptosis. Where in this cascade of events ERp57 plays a role remains to be determined.

ERp57 in aggresomes

A common thread for many neurodegenerative disorders is the accumulation of misfolded proteins (33). In general, misfolded proteins are handled by the ubiquitin–proteosome system. If overwhelmed, however, ER stress and UPR are triggered. Similarly, autophagy is also thought to be a cellular defense system. A conceivable point of convergence is suggested by studies showing that if autophagic degradation is not rapid enough or is insufficient in some way, ER stress and UPR may be initiated. Aggresome formation is thought to contribute to autophagy by concentrating substrates in one area for more efficient disposal. Surprisingly, we have not observed aggresome formation in previous studies in either MN9D cells or primary dopaminergic neurons. Nor did we observe aggresomes when the major component of Lewy bodies, α-synuclein, was overexpressed in either its wild-type or mutant forms (18). Whether the doughnut-shaped structures (see Fig. 5) formed by ERp57 and cytochrome *c* are *bona fide* aggresomes is unclear at present. Several hallmarks of aggresomes are missing, such as clustering around a microtubule-organizing center (data not shown). However, LAMP1 immunoreactivity at the core of the structure (see Fig. 6) is suggestive of early accumulation of lysosomes near the nucleus and the formation of aggresome-like structures.

Many studies have documented the association of chaperones with protein aggregates. Some of the most compelling evidence comes from studies showing that HSP70 can overcome many disease-causing aggregates such as polyglutamine aggregates or α-synuclein aggregates (27). Whether the ERp57-forming aggregates are derived from the cytoplasm or from recruitment of mitochondria is unknown. However, it seems reasonable to suggest that they represent the latter organelle, because so little of this protein is free in the cytosol in dopaminergic cells (see Fig. 3A). Moreover, the finding that ERp57 staining colocalizes with cytochrome *c* before its loss from mitochondria agrees with recent data showing the presence of intact mitochondria in aggresomes (28, 45). Indeed, Waelter *et al.* (45) hypothesized that mitochondria were recruited into aggresomes to provide the energy necessary for protein degradation. Results from this laboratory are consistent with this notion, because the complex I inhibitor, MPP^+, does not induce aggresome formation in this system (not shown).

The significance of ERp57 in aggresomes remains unclear. Although it may simply represent a passively recruited protein, the formation of HMW conjugates of mitochondrial DNA (see Fig. 4D) suggests a more active, adaptive response. Taken together, these data suggest that 6-OHDA–generated ROS activates UPR by oxidizing, among other proteins, ERp57. These changes trigger adaptive cellular responses that, because of prolonged toxin-mediated stress, eventually lead to cell death. Understanding the signaling mechanisms associated with parkinsonian mimetics as well as their temporal induction may aid in designing better interventions in models of PD.

ACKNOWLEDGMENTS

We thank Dr. Yuh-Jiin I. Jong and Mr. Steve Harmon for technical assistance. This work was supported by NIH grant NS39084, MH45330.

ABBREVIATIONS

6-OHDA, 6-hydroxydopamine; AMS, 4-acetamido-4′-maleimidylstilbene-2,2′-disulfonic acid; DPS, dipyridyl sulfide; DTT, dithiothreitol; ER, endoplasmic reticulum; HMW, high molecular weight; MAM, mitochondria-associated membrane; MPP+, 1-methyl-4-phenylpyridinium; NAC, *N*-acetyl-L-cysteine; NEM, *N*-ethylmaleimide; PBS, phosphate-buffered saline; PD, Parkinson's disease; PDI, protein disulfide iso-

merases; PDIA3, protein disulfide isomerase–associated protein 3; PNGF, peptide:*N*-glycosidase F; ROS, reactive oxygen species; Rot, rotenone; TH, tyrosine hydroxylase; UPR, unfolded protein response.

REFERENCES

1. Beal MF. Oxidatively modified proteins in aging and disease. *Free Radic Biol Med* 32: 797–803, 2002.
2. Celli CM and Jaiswal AK. Role of GRP58 in mitomycin C-induced DNA cross-linking. *Cancer Res* 63: 6016–6025, 2003.
3. Chichiarelli S, Ferraro A, Altieri F, Eufemi M, Coppari S, Grillo C, Arcangeli V, and Turano C. The stress protein ERp57/GRP58 binds specific DNA sequences in HeLa cells. *J Cell Physiol* 210: 343–351, 2007.
4. Choi HK, Won L, Roback JD, Wainer BH, and Heller A. Specific modulation of dopamine expression in neuronal hybrid cells by primary cells from different brain regions. *Proc Natl Acad Sci U S A* 89: 8943–8947, 1992.
5. Choi J, Malakowsky CA, Talent JM, Conrad CC, Carroll CA, Weintraub ST, and Gracy RW. Anti-apoptotic proteins are oxidized by Abeta25-35 in Alzheimer's fibroblasts. *Biochim Biophys Acta* 1637: 135–141, 2003.
6. Coppari S, Altieri F, Ferraro A, Chichiarelli S, Eufemi M, and Turano C. Nuclear localization and DNA interaction of protein disulfide isomerase ERp57 in mammalian cells. *J Cell Biochem* 85: 325–333, 2002.
7. Dalle-Donne I, Giustarini D, Colombo R, Rossi R, and Milzani A. Protein carbonylation in human diseases. *Trends Mol Med* 9: 169–176, 2003.
8. Falcon-Perez JM, Nazarian R, Sabatti C, and Dell'Angelica EC. Distribution and dynamics of Lamp1-containing endocytic organelles in fibroblasts deficient in BLOC-3. *J Cell Sci* 118: 5243–5255, 2005.
9. Ferger B, Rose S, Jenner A, Halliwell B, and Jenner P. 6-Hydroxydopamine increases hydroxyl free radical production and DNA damage in rat striatum. *Neuroreport* 12: 1155–1159, 2001.
10. Frickel EM, Frei P, Bouvier M, Stafford WF, Helenius A, Glockshuber R, and Ellgaard L. ERp57 is a multifunctional thiol-disulfide oxidoreductase. *J Biol Chem* 279: 18277–18287, 2004.
11. Hardy J, Cai H, Cookson MR, Gwinn-Hardy K, and Singleton A. Genetics of Parkinson's disease and parkinsonism. *Ann Neurol* 60: 389–398, 2006.
12. Hetz C, Russelakis-Carneiro M, Walchli S, Carboni S, Vial-Knecht E, Maundrell K, Castilla J, and Soto C. The disulfide isomerase Grp58 is a protective factor against prion neurotoxicity. *J Neurosci* 25: 2793–802, 2005.
13. Holtz WA and O'Malley KL. Parkinsonian mimetics induce aspects of unfolded protein response in death of dopaminergic neurons. *J Biol Chem* 278: 19367–19377, 2003.
14. Holtz WA, Turetzky JM, Jong YJ, and O'Malley KL. Oxidative stress-triggered unfolded protein response is upstream of intrinsic cell death evoked by parkinsonian mimetics. *J Neurochem* 99: 54–69, 2006.
15. Holtz WA, Turetzky JM, and O'Malley KL. Microarray expression profiling identifies early signaling transcripts associated with 6-OHDA-induced dopaminergic cell death. *Antioxid Redox Signal* 7: 639–648, 2005.
16. Iwata A, Riley BE, Johnston JA, and Kopito RR. HDAC6 and microtubules are required for autophagic degradation of aggregated huntingtin. *J Biol Chem* 280: 40282–40292, 2005.
17. Izumi Y, Sawada H, Sakka N, Yamamoto N, Kume T, Katsuki H, Shimohama S, and Akaike A. p-Quinone mediates 6-hydroxydopamine-induced dopaminergic neuronal death and ferrous iron accelerates the conversion of p-quinone into melanin extracellularly. *J Neurosci Res* 79:849–860, 2005.
18. Jensen PJ, Alter BJ, and O'Malley KL. Alpha-synuclein protects naive but not dbcAMP-treated dopaminergic cell types from 1-methyl-4-phenylpyridinium toxicity. *J Neurochem* 86: 196–209, 2003.
19. Jessop CE and Bulleid NJ. Glutathione directly reduces an oxidoreductase in the endoplasmic reticulum of mammalian cells. *J Biol Chem* 279: 55341–55347, 2004.
20. Jessop CE, Chakravarthi S, Watkins RH, and Bulleid NJ. Oxidative protein folding in the mammalian endoplasmic reticulum. *Biochem Soc Trans* 32: 655–658, 2004.
21. Kopito RR. Aggresomes, inclusion bodies and protein aggregation. *Trends Cell Biol* 10: 524–530, 2000.
22. Laragione T, Gianazza E, Tonelli R, Bigini P, Mennini T, Casoni F, Massignan T, Bonetto V, and Ghezzi P. Regulation of redox-sensitive exofacial protein thiols in CHO cells. *Biol Chem* 387: 1371–1376, 2006.
23. Lee AS, Delegeane A, and Scharff D. Highly conserved glucose-regulated protein in hamster and chicken cells: preliminary characterization of its cDNA clone. *Proc Natl Acad Sci U S A* 78: 4922–4925, 1981.
24. Levay G, Ye Q, and Bodell WJ. Formation of DNA adducts and oxidative base damage by copper mediated oxidation of dopamine and 6-hydroxydopamine. *Exp Neurol* 146: 570–574, 1997.
25. Lotharius J, Dugan LL, and O'Malley KL. Distinct mechanisms underlie neurotoxin-mediated cell death in cultured dopaminergic neurons. *J Neurosci* 19:1284–1293, 1999.
26. Melero JA and Smith AE. Possible transcriptional control of three polypeptides which accumulate in a temperature-sensitive mammalian cell line. *Nature* 272: 725–727, 1978.
27. Meredith SC. Protein denaturation and aggregation: cellular responses to denatured and aggregated proteins. *Ann N Y Acad Sci* 1066: 181–221, 2005.
28. Muqit MM, Abou-Sleiman PM, Saurin AT, Harvey K, Gandhi S, Deas E, Eaton S, Payne Smith MD, Venner K, Matilla A, Healy DG, Gilks WP, Lees AJ, Holton J, Revesz T, Parker PJ, Harvey RJ, Wood NW, and Latchman DS. Altered cleavage and localization of PINK1 to aggresomes in the presence of proteasomal stress. *J Neurochem* 98: 56–69, 2006.
29. Nagata E, Sawa A, Ross CA, and Snyder SH. Autophagosome-like vacuole formation in Huntington's disease lymphoblasts. *Neuroreport* 15: 1325–1328, 2004.
30. Ndubuisi MI, Guo GG, Fried VA, Etlinger JD, and Sehgal PB. Cellular physiology of STAT3: where's the cytoplasmic monomer? *J Biol Chem* 274: 25499–25509, 1999.
31. Nixon RA. Autophagy in neurodegenerative disease: friend, foe or turncoat? *Trends Neurosci* 29: 528–535, 2006.
32. Nystrom T. Role of oxidative carbonylation in protein quality control and senescence. *EMBO J* 24: 1311–1317, 2005.
33. Paschen W and Mengesdorf T. Endoplasmic reticulum stress response and neurodegeneration. *Cell Calcium* 38: 109–115, 2005.
34. Reverter-Branchat G, Cabiscol E, Tamarit J, and Ros J. Oxidative damage to specific proteins in replicative and chronological-aged *Saccharomyces cerevisiae*: common targets and prevention by calorie restriction. *J Biol Chem* 279: 31983–31989, 2004.
35. Rideout HJ, Lang-Rollin I, and Stefanis L. Involvement of macroautophagy in the dissolution of neuronal inclusions. *Int J Biochem Cell Biol* 36: 2551–2562, 2004.
36. Ryu EJ, Angelastro JM, and Greene LA. Analysis of gene expression changes in a cellular model of Parkinson disease. *Neurobiol Dis* 18: 54–74, 2005.
37. Ryu EJ, Harding HP, Angelastro JM, Vitolo OV, Ron D, and Greene LA. Endoplasmic reticulum stress and the unfolded protein response in cellular models of Parkinson's disease. *J Neurosci* 22: 10690–10698, 2002.
38. Saito Y, Nishio K, Ogawa Y, Kinumi T, Yoshida Y, Masuo Y, and Niki E. Molecular mechanisms of 6-hydroxydopamine-induced cytotoxicity in PC12 cells: involvement of hydrogen peroxide-dependent and -independent action. *Free Radic Biol Med* 42: 675–685, 2007.
39. Sekine Y, Takeda K, and Ichijo H. The ASK1-MAP kinase signaling in ER stress and neurodegenerative diseases. *Curr Mol Med* 6: 87–97, 2006.
40. Sharma M and Slocum HK. Prevention of quinone-mediated DNA arylation by antioxidants. *Biochem Biophys Res Commun* 262: 769–774, 1999.
41. Stokes AH, Hastings TG, and Vrana KE. Cytotoxic and genotoxic potential of dopamine. *J Neurosci Res* 55: 659–665, 1999.

42. Stone SJ and Vance JE. Phosphatidylserine synthase-1 and -2 are localized to mitochondria-associated membranes. *J Biol Chem* 275: 34534–34540, 2000.
43. Szegezdi E, Logue SE, Gorman AM, and Samali A. Mediators of endoplasmic reticulum stress-induced apoptosis. *EMBO Rep* 7: 880–885, 2006.
44. Turano C, Coppari S, Altieri F, and Ferraro A. Proteins of the PDI family: unpredicted non-ER locations and functions. *J Cell Physiol* 193: 154–163, 2002.
45. Waelter S, Boeddrich A, Lurz R, Scherzinger E, Lueder G, Lehrach H, and Wanker EE. Accumulation of mutant huntingtin fragments in aggresome-like inclusion bodies as a result of insufficient protein degradation. *Mol Biol Cell* 12: 1393–1407, 2001.
46. Wang P, Song Y, Zhang L, He H, and Zhou X. Quinone methide derivatives: important intermediates to DNA alkylating and DNA cross-linking actions. *Curr Med Chem* 12: 2893–2913, 2005.
47. Wang X, Thomas B, Sachdeva R, Arterburn L, Frye L, Hatcher PG, Cornwell DG, and Ma J. Mechanism of arylating quinone toxicity involving Michael adduct formation and induction of endoplasmic reticulum stress. *Proc Natl Acad Sci U S A* 103: 3604–3609, 2006.
48. Williams DB. Beyond lectins: the calnexin/calreticulin chaperone system of the endoplasmic reticulum. *J Cell Sci* 119: 615–623, 2006.

Address reprint requests to:
Karen L. O'Malley, Ph.D.
Department of Anatomy and Neurobiology
660 S. Euclid Avenue (Box 8108)
Washington University School of Medicine
St. Louis, MO 63110

E-mail: omalleyk@wustl.edu

Date of first submission to ARS Central, June 18, 2007; date of acceptance, June 23, 2007.

This article has been cited by:

1. Catherine I. Andreu, Ute Woehlbier, Mauricio Torres, Claudio Hetz. 2012. Protein disulfide isomerases in neurodegeneration: From disease mechanisms to biomedical applications. *FEBS Letters* **586**:18, 2826-2834. [CrossRef]
2. Umamaheswari Ramachandran, Arulmani Manavalan, Husvinee Sundaramurthi, Siu Kwan Sze, Zhi Wei Feng, Jiang-Miao Hu, Klaus Heese. 2012. Tianma modulates proteins with various neuro-regenerative modalities in differentiated human neuronal SH-SY5Y cells. *Neurochemistry International* **60**:8, 827-836. [CrossRef]
3. XJ Zhao, RZ Tang, ML Wang, WL Guo, J Liu, L Li, WJ Xing. 2012. Distribution of PDIA3 transcript and protein in rat testis and sperm cells. *Reproduction in Domestic Animals* no-no. [CrossRef]
4. Carlo Turano, Elisa Gaucci, Caterina Grillo, Silvia Chichiarelli. 2011. ERp57/GRP58: A protein with multiple functions. *Cellular & Molecular Biology Letters* . [CrossRef]
5. Micha M. M. Wilhelmus, Robin Verhaar, Gerda Andringa, John G. J. M. Bol, Patrick Cras, Ling Shan, Jeroen J. M. Hoozemans, Benjamin Drukarch. 2011. Presence of Tissue Transglutaminase in Granular Endoplasmic Reticulum is Characteristic of Melanized Neurons in Parkinson's Disease Brain. *Brain Pathology* **21**:2, 130-139. [CrossRef]
6. LX Lv, B Ujisguleng, B Orhontana, WB Lian, WJ Xing. 2011. Molecular Cloning of Sheep and Cashmere Goat Pdia3 and Localization in Sheep Testis. *Reproduction in Domestic Animals* no-no. [CrossRef]
7. Marzia Perluigi, Fabio Di Domenico, Carla Blarzino, Cesira Foppoli, Chiara Cini, Alessandra Giorgi, Caterina Grillo, Federico De Marco, David A Butterfield, Maria E Schinin#, Raffaella Coccia. 2010. Effects of UVB-induced oxidative stress on protein expression and specific protein oxidation in normal human epithelial keratinocytes: a proteomic approach. *Proteome Science* **8**:1, 13. [CrossRef]
8. Martin Schröder , Kenji Kohno . 2007. Recent Advances in Understanding the Unfolded Protein Response. *Antioxidants & Redox Signaling* **9**:12, 2241-2244. [Citation] [Full Text PDF] [Full Text PDF with Links]